Numerical construction of the GGE in integrable models: A Hilbert space Monte Carlo approach

Vincenzo Alba[1] and Maurizio Fagotti[2]

[1]*International School for Advanced Studies (SISSA), Via Bonomea 265, 34136, Trieste, Italy, INFN, Sezione di Trieste*
[2]*Département de Physique, Ecole normale superieure, CNRS, 24 rue Lhomond, 75005 Paris, France*

(Dated: July 3, 2015)

I. INTRODUCTION

The issue of how statistical ensembles emerge from the out-of-equilibrium dynamics in *isolated* quantum many-body system is still a fundamental, yet challenging, problem. Much of the motivation for the renewed interest in this topic originated from the high degree of control reached in out-of-equilibrium expriments with cold atomic gases. The paradigm of out-of-equilibrium experiment is the quantum quench, in which a system is initially prepared in some eigenstate $|\Psi_0\rangle$ of a many-body Hamiltonian. Then a parameter in the Hamiltonian is suddenly changed, and the system is let to evolve unitarily.

While at long times after the quench the system is expected to equilibrate, in one dimensional integrable systems the presence of non-trivial local conserved quantities besides the energy strongly affects the dynamics and the steady state at long times. Thus the question as to wheather steady-state properties can be described by a statistical ensemble and how to construct it is still open.

There is compelling evidence that the steady state expectation values of a generic local operator $\mathcal{O}$ are described by a Generalized Gibbs Ensemble (GGE) as $\langle\mathcal{O}\rangle \equiv \mathrm{Tr}(\mathcal{O}\rho^{GGE})/Z$ with Z a normalization constant. The GGE density matrix ρ^{GGE} extends the Gibbs density matrix by including (in principle) all the integrals of motion $\mathcal{I}_j$ as

$$\rho^{GGE} = Z^{-1}\exp\big(-\lambda_j\mathcal{I}_j\big), \tag{1}$$

where we assume summation over the repeated index j, and λ_j are Lagrange multipliers to be fixed by imposing $\langle\Psi_0|\mathcal{I}_j|\Psi_0\rangle = \langle\mathcal{I}_j\rangle$. In practice, in realistic situations one deals with the truncated GGE (tGGE), which is obtained by considering only a finite number of *local* integral of motion.

The validity of the GGE has been largely confirmed in non interacting field theories. In interacting models the scenario is not clear. Recently, a lot of insights came from the the so-called Quench Action method, which allows to calculate steady state properties in Bethe ansatz solvable models, provided that the overlap between $|\Psi_0\rangle$ and the eigenstates of the model are known.

Surprisingly, it has been observed that in the spin-$\frac{1}{2}$ Heisenberg XXZ spin chain, for the quench starting with the Neel state steady state properties are not correctly described by the TGGE, while they are in perfect agreement with the quench action method.

While one might argue that the GGE can be repaired by including more conserved quantities, as to now no quantitative study has been conducted yet. One intriguing possibility is that quasi-local charges are needed, although no systematic attempt of including them has been made.

On the numerical side, time dependent DMRG gives the possibility to simulate the dynamics of quantum many body systems for short times, althugh is some cases this is sufficient to address steady state properties. However, no numerical attempt of exploring the GGE itself and possible extensions has been proposed yet.

We provide a numerical Monte-Carlo-based framework to simulate and extend the GGE.

The method is deviced for finite-size Bethe ansatz solvable models, although thermodynamic quantities can be obtained by standard finite-size scaling analysis. The method relies on the knowledge of the Hilbert space of the model and the so-called Bethe-Takahashi equations. Moreover, it is restricted to observables for which the corresponding expression in terms of the B-T roots (rapidities) is known.

The method allows to address local observables for which the expression in terms of the rapidity is known as well.

The basic idea is to sample the Hilbert space of the model according to the desired ensemble. Notice that for the Gibbs ensemble this idea has been explored in Ref. 121.

Remarkably, this allows to extract the rapidity densities defining the ensemble representative state in the thermodynamic limit.

Finite-size effects are under control and for moderately large chain sizes the Monte Carlo results agree very well with the thermodynamic limit results, especially for small rapidities. Higher rapidities are more sensitive to finite size effects as they reflec short length scales.

An alternative numerical method would be Quantum Monte Carlo. However, this would require the implementation of the higher conserved charges, other than the Hamiltonian. As the range of higher charges becomes large this is not easily doable in practice.

We provide the first numerical verification of the validity of the GTBA equations for the Heisenberg spin chain.

Interestingly, finite-size corrections are generically small, i.e., expontially decaying with the chain size.

Our Monte Carlo approach can be trivially extended to include other conserved charges, both local and non-local, and arbitrary functions of the rapidities. While the former is related to the GGE average of the particle number, the latter measures its fluctuations. Notice that due to the $SU(2)$ symmetry of the conserved charges one has that $\langle S_z\rangle = 0$ (panel (g)).

II. THE HEISENBERG SPIN CHAIN

The isotropic spin-$\frac{1}{2}$ Heisenberg (XXX) chain is defined by the Hamiltonian

$$\mathcal{H} \equiv J \sum_{i=1}^{L} \left[\frac{1}{2}(S_i^+ S_{i+1}^- + S_i^- S_{i+1}^+) + S_i^z S_{i+1}^z \right], \quad (2)$$

where $S_i^{\pm} \equiv (\sigma_i^x \pm i\sigma_i^y)/2$ are spin operators acting on the site i of the chain, $S_i^z \equiv \sigma_i^z/2$, and $\sigma_i^{x,y,z}$ the Pauli matrices. We fix $J = 1$ and use periodic boundary conditions identifying sites $L+1$ and 1. The total magnetization $S_T^z \equiv \sum_i S_i^z = L/2 - M$, with M number of down spins (particles), commute with (2). Thus, the eigenstates of (2) can be labelled by M.

In the Bethe ansatz framework each eigenstate of (2) is univocally identified by a set of M complex parameters (so-called rapidities) $\{x_\alpha \in \mathbb{C}\}_{\alpha=1}^M$. In the thermodynamic limit $L \to \infty$ the rapidities x_α form "string" patterns along the imaginary direction in the complex plane (string hypothesis). The rapidities forming a string of length $1 \leq n \leq M$ (so-called n-string) are parametrized as $x_{n;\gamma}^{(j)} = x_{n;\gamma} - i(n-1-2j), \quad j = 0, 1, \ldots, n-1,$, where $x_{n;\gamma} \in \mathbb{R}$ is the real part of the string (string center), j labels the different rapidities in the same n-string, andγ denotes strings of the same length but with different centers. Although the string hypothesis is not correct for finite chains, deviations typically, i.e., for most of the eigenstates, decay exponentially with system size. Physically, the n-strings correspond to eigenstate components containing bound states of n particles. The string centers $x_{n;\gamma}$ are solutions of the Bethe-Takahashi equations

$$L\vartheta_n(x_{n;\gamma}) = 2\pi I_{n;\gamma} + \sum_{(m,\beta)\neq(n,\gamma)} \Theta_{m,n}(x_{n;\gamma} - x_{m;\beta}). \quad (3)$$

Here $\vartheta_n(x) \equiv 2\arctan(x/n)$, $\Theta_{m,n}(x)$ is the scattering phase between different rapidities, and $I_{n;\gamma} \in \frac{1}{2}\mathbb{Z}$ are the so-called Bethe-Takahashi quantum numbers. The $I_{n;\gamma}$ obey the upper bound $|I_{n;\gamma}| \leq I_{\text{MAX}}(n, L, M)$, with I_{MAX} a known function of n, M, L. Every choice of $I_{n;\gamma}$ identifies an eigenstate of (2). Notice that each eigenstate contains strings of different lengths. We define the "string content" of an eigenstate as $\mathcal{S} \equiv \{s_1, \ldots, s_M\}$, with $0 \leq s_n \leq \lfloor M/n \rfloor$ the number of n-strings. By definition one has $\sum_j j s_j = M$.

Besides the total magnetization and the momentum, the XXX chain has non-trivial *local* conserved charges $\mathcal{I}_j$, with $[\mathcal{I}_j, \mathcal{I}_k] = 0 \, \forall j, k$. These are obtained as

$$\mathcal{I}_{j+1} \equiv \frac{i}{(j-1)!} \frac{d^j}{dy^j} \log(\Lambda(\{x_{n;\gamma}\}, y))\Big|_{y=i}. \quad (4)$$

Here Λ in the Algebraic Bethe ansatz is the eigenvalue of the quantum transfer matrix $T(y)$, with y the spectral parameter. The dependence of Λ on the rapidities $x_{n;\gamma}$ is known. One can check that $\mathcal{I}_2 = \mathcal{H}$. The range of $\mathcal{I}_j$ increases linearly with j, i.e., larger j correspond to less local charges. Remarkably, the eigenvalues of $\mathcal{I}_j$ over a generic eigenstate are obtained by summing the contributions of the different string sectors independently. For instance, the energy is obtained as $E = \sum_n E_n$, where $E_n = 2\sum_\gamma n/(n^2 + x_{n;\gamma}^2)$.

III. HILBERT SPACE MONTE CARLO SAMPLING

For a finite chain the GGE ensemble can be generated by sampling the eigenstates of (2) with the probability (1). This can be done efficiently using Monte Carlo. One starts with an initial M particle eigenstate of (2), with string content $\mathcal{S} = \{s_1, \ldots, s_M\}$, identified by Bethe-Takahashi quantum number configuration $\mathcal{C} = \{I_{n;\gamma}\}_{n=1}^M$ ($\gamma = 1, \ldots, s_n$). Let us denote the expectation values of the conserved charges as $\{\mathcal{I}_j\}$. The basic idea is to generate a new eigenstate with a Metropolis update. Specifically, each Monte Carlo step (mcs) consists of three moves:

1. Choose a new particle number sector M' and a string content $\mathcal{S}'$ with probability $P(M', \mathcal{S}')$.

2. Generate a quantum number configuration $\mathcal{C}'$ compatible with the $\mathcal{S}'$ obtained in step 1 and solve the Bethe-Takahashi equations (3) to extract the new rapidities $\{x_{n;\gamma}\}$.

3. After calculating the expctation values of the charges $\mathcal{I}_j'$ accept the new eigenstate with the Metropolis probability:

$$\text{Min}\left(1, \frac{L-2M'+1}{L-2M+1} e^{-\sum_j \lambda_j(\mathcal{I}_j' - \mathcal{I}_j)}\right). \quad (5)$$

In (5) the factor in front of the exponential takes into account that eigenstates in the same $SU(2)$ mutliplet have the same charges expectation value, i.e., the $\mathcal{I}_j$ are $SU(2)$ scalars. Crucially, the steps 1 and 2 are necessary in order to account for the density of states of the Heisenberg spin chain. The steps $1-3$ define a Markov chain, which, after a thermalization, generates eigenstates sampled according to (1). Notice that it is straighforward to extend the algorithm to consider fixed particle number M. More interestingly, by trivially modifying (5) it is possible to simulate more exotic ensembles in whichl instead of the charges $\mathcal{I}_j$, one conseiders arbitrary functions of the rapidities. For instance, this would be useful in order to explore the effect of quasi-local charge on the GGE.

We should mention that a similar method has been developed in Ref... to construct the the Gibbs ensemble in the Heisenberg spin chain.

The GGE expectation values $\langle\mathcal{O}\rangle$ are as the average of the expectation values of $\mathcal{O}$ over the eigenstates $|\{x_{n;\gamma}\}\rangle$ generated by the Monte Carlo as

$$\langle\mathcal{O}\rangle = \lim_{N_{\text{mcs}}\to\infty} \frac{1}{N_{\text{mcs}}} \sum_{\{x_{n;\gamma}\}} \langle\{x_{n;\gamma}\}|\mathcal{O}|\{x_{n;\gamma}\}\rangle, \quad (6)$$

where N_{mcs} is the number of Monte Carlo steps, i.e. the number of eigenstates in the sum.

IV. GGE FOR LOCAL OBSERVABLES

The validity of the Monte Carlo method is illustrated in Fig. 3 considering the GGE expectation values of the charge

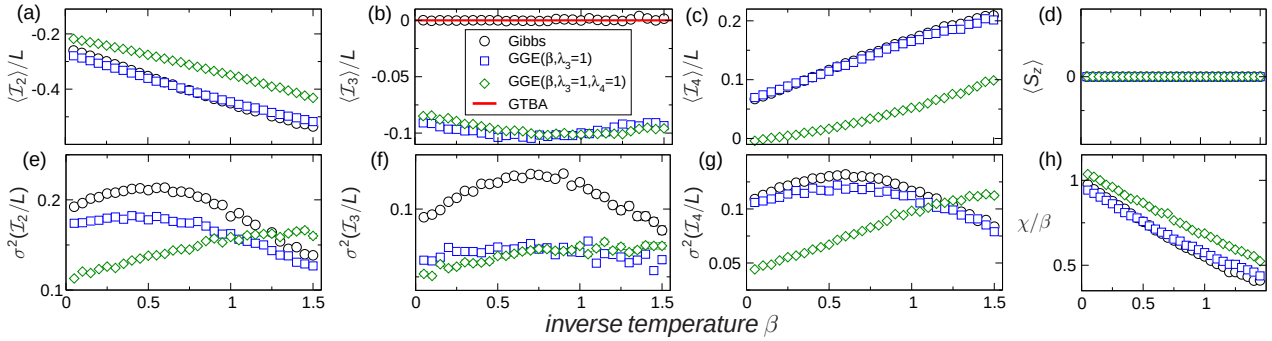

FIG. 1. The Generalized Gibbs Ensemble (GGE) for the Heisenberg spin chain with $L = 16$ sites: numerical results obtained using the Hilbert space Monte Carlo sampling. Only the first three conserved charges $\mathcal{I}_n$ ($n = 1, 2, 3$), with associated Lagrange multipliers λ_n, are included in the GGE. Here $\mathcal{I}_2$ is the Hamiltonian and $\lambda_2 \equiv \beta$ the inverse temperature. In all the panels different symbols correspond to different values of λ_3, λ_4. The circles correspond to the Gibbs ensemble, i.e., $\lambda_3 = \lambda_4 = 0$. (a) The GGE average $\langle \mathcal{I}_2/L \rangle$ plotted as a function of β. (b) Variance of the GGE fluctuations $\sigma^2(\mathcal{I}_2/L) \equiv \langle (\mathcal{I}_2/L)^2 \rangle - \langle \mathcal{I}_2/L \rangle^2$ as a function of β. (c)(d) and (e)(f): Same as in (a)(b) for $\mathcal{I}_3$ and $\mathcal{I}_4$, respectively. In all panels the dash-dotted lines are the analytical results obtained using the Generalized Thermodynamic Bethe Ansatz (GTBA). (g) The GGE expectation value of the total magnetization $\langle S_z \rangle$. Notice that $\langle S_z \rangle = 0$ due to the $SU(2)$ invariance of the conserved charges. (h) χ/β plotted versus β, with χ being the magnetic susceptibility per site.

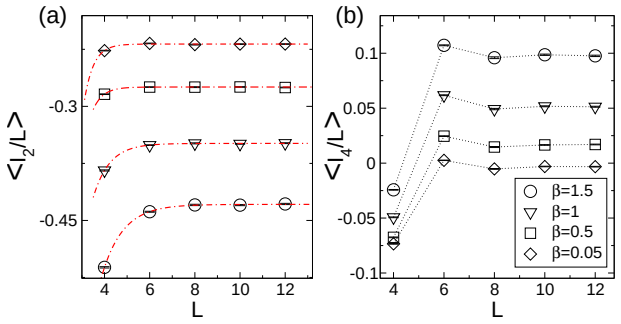

FIG. 2. Finite-size scaling of the GGE averages in the Heisenberg chain: Numerical results obtained from the Hilbert space Monte Carlo sampling. Here the GGE is constructed including $\mathcal{I}_2, \mathcal{I}_3, \mathcal{I}_4$, with Lagrange multipliers $\lambda_2 = \beta, \lambda_3 = \lambda_4 = 1$. (a) $\langle \mathcal{I}_2/L \rangle$ plotted versus the chain size L for several values of β. The dash-dotted lines are exponential fits. (b) Same as in (a) for $\mathcal{I}_4$.

densities $\langle \mathcal{I}_j/L \rangle$ (panels (a)-(c) in the Figure) and the variance of their ensemble fluctuations $\sigma^2(\mathcal{I}_j) \equiv \langle \mathcal{I}_j^2 \rangle - \langle \mathcal{I}_j \rangle^2$ (panels (d)-(f)). Finally, panels (g)(h) plot the total magnetization $\langle S_z \rangle$ (i.e., the particle number) and the spin susceptibility χ (particle number fluctutations). Notice that $\sigma^2(\mathcal{I}_2)$ is related to the specific heat, $\mathcal{I}_3 \equiv \sum_{\alpha\beta\gamma} \epsilon_{\alpha\beta\gamma} \sigma_i^\beta \sigma_{i+1}^\gamma \sigma_{i+2}^\alpha$ is the energy current, and $\sigma^2(\mathcal{I}_3)$ is related to the energy Drude weight. Here the data are for the truncated TGGE constructed with the first three charges $\mathcal{I}_2, \mathcal{I}_3, \mathcal{I}_4$. We consider several values of the Lagrange multipliers, namely $\lambda_3 = \lambda_4 = 0$ (Gibbs ensemble, circles in the Figure), $\lambda_3 = 1$ and $\lambda_4 = 0$ (squares), and $\lambda_3 = \lambda_4 = 1$ (rhombi). All our results are plotted versus the inverse temperature $\lambda_2 = \beta$. The data are Monte Carlo results for $N_{\rm mcs} = 5 \cdot 10^5$. In most of the cases, especially for small β the Monte Carlo error bars are small than the symbols. As expected, the different ensemble give different expectation values, implying that the local observables we consider are able to distinguish different GGEs. Notice that in panel (b) $\langle \mathcal{I}_3 \rangle = 0$ for the Gibbs ensemble due to the parity invariance of $\mathcal{I}_j$ with even j, while in (d) $\langle S_z \rangle = 0$ due to the $SU(2)$ symmetry of (2). In all the panels in Fig. 3 the continuous lines are the analyitic results obtained in the thermodynamic limit by solving the $GTBA$ equations. These which fully match the Monte Carlo data, which signals that the finite-size effects are negligible already for $L = 16$, at least for the values of the λ_j considered.

The finite-size corrections are more carefully investigated in Fig. 2. Fig. 2 plots $\langle \mathcal{I}_2 \rangle$ and $\langle \mathcal{I}_4 \rangle$ (panels (a) and (b), respectively) versus β. Here we focus on the $TGGE$ with $\lambda_2 = \beta, \lambda_3 = 0$ and $\lambda_4 = 1$. Panel (a) demonstrates that finite-size effects decay exponentially with L for any β. Clearly, corrections are larger at lower temperature, as expected. Moreover, they increase with the range of the operator as shown in panel (b), although the behavior remains exponential.

V. EXTRACTING THE RAPIDITY DENSITIES

In the thermodynamic limit in each n-string sector the roots of (3) become dense. Thus, each eigenstate is characterized by the root distribution $\boldsymbol{\rho} \equiv \{\rho_n\}_{n=1}^\infty$. Formally, the ρ_n are defined as $\rho_n = \lim_{L\to\infty} [L(x_{n;\gamma+1} - x_{n;\gamma})]^{-1}$. For a generic observable $\mathcal{O}$, the GGE average becomes a functional integral as

$$\mathrm{Tr}\{ \exp(\lambda_j \mathcal{I}_j) \mathcal{O} \} \to \int \mathcal{D}\boldsymbol{\rho} \exp\big(S[\boldsymbol{\rho}] + \lambda_j \mathcal{I}_j[\boldsymbol{\rho}]\big) \mathcal{O}[\boldsymbol{\rho}]. \quad (7)$$

Here $S[\boldsymbol{\rho}]$ is the Yang-Yang entropy. $S[\boldsymbol{\rho}]$ counts the number of eigenstates leading to the same $\boldsymbol{\rho}$, and it is extensive. In (7) $\mathcal{O}$ is assumed that $\mathcal{O}$ becomes a smooth function of $\boldsymbol{\rho}$ in the thermodynamic limit. Since both S and $\mathcal{I}_j$ are extensive, the integral in (7) is dominated by the saddle point $\boldsymbol{\rho}^{sp}$, with $\delta(S + \lambda_j \mathcal{I}_j)/\delta\boldsymbol{\rho}|_{\boldsymbol{\rho}=\boldsymbol{\rho}^{sp}} = 0$. Here $\boldsymbol{\rho}^{sp}$ acts as a representative state for the ensemble, and it contains the full information about

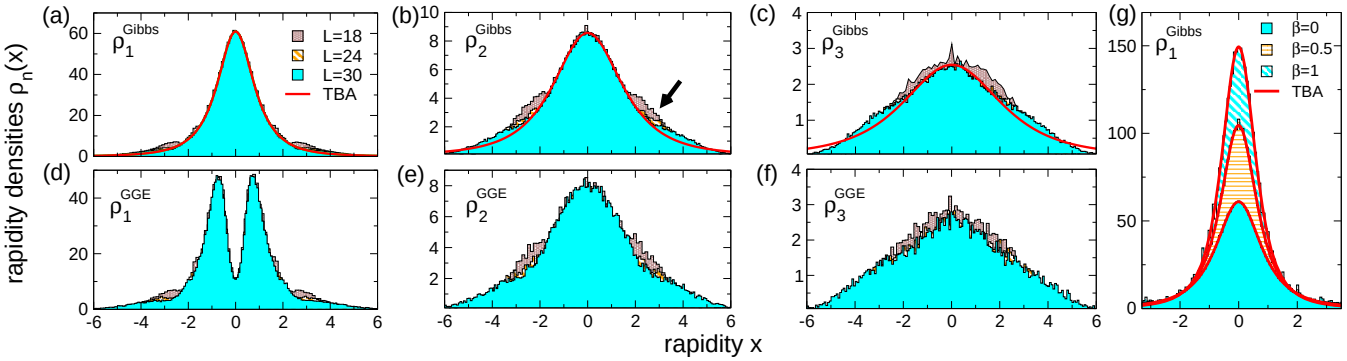

FIG. 3. The rapidity densities $\rho_n(x)$ (for $n = 1, 2, 3$) for the infinite temperature Gibbs (panels (a)-(c)) and the GGE equilibrium states (panels (d)-(f)): Numerical results for the Heisenberg spin chain obtained using the Hilbert space Monte Carlo sampling. Here the GGE is constructed including only $\mathcal{I}_2$ and $\mathcal{I}_4$ with fixed Lagrange multipliers $\lambda_2 = 0$ and $\lambda_4 = 1$. In all the panels the data are the histograms of the n-strings rapidities sampled in the Monte Carlo. The width of the histogram bins is $\Delta x = 2/L$. In each panel different histograms correspond to different chain sizes L. All the histograms are divided by 10^3 for convenience. In (b) the arrow is to highlight the finite-size effects. In panels (a)-(c) the lines are the Thermodynamic Bethe Ansatz (TBA) results. (g) Finite-temperature effects: Monte Carlo data for ρ_1^{Gibbs} for different values of the inverse temperature β.

the GGE equilibrium steady state. Eq. (6) suggests/implies that the representative state root densities ρ_n^{sp} can be obtained the histograms of the roots $x_{n;\gamma}$ sampled in the Monte Carlo history, in the limit $L \to \infty$.

This is supported in Fig. 3 considering several GGEs. Panels (a)-(c) plot the root densities $\rho_n^{sp}(x)$ for $n = 1, 2, 3$ as a function of x for the representative state (saddle point) of the infinite-temperature Gibbs ensemble. In each panel the different histograms correspond to different chain sizes $18 \leq L \leq 30$. The data are obtained from Monte Carlo histories with $4 \cdot 10^5$ Monte Carlo steps. The width of the histogram bins is varied with che chain size as $2/L$. In all the panels the full lines are the analytic results obtained from the Thermodynamic Bethe Ansatz (TBA) (cf. (10)). Remarkably, the Monte Carlo data are in good agreement with the TBA results. This agreement is perfect for $n = 1$, whereas it become progressively worse upon considering larger $n > 1$ (see panels (b)(c)). Clearly, the deviations from the TBA result vanish upon increasing the system size (see for instance the arrow in panel (b)). These finite-size effects are larger on the tails of the distributions. This is expected since large rapidities correspond to large quasi-momenta, which are more sensitive to the lattice effects. Finally, finite-size effects increase with n, i.e., with the bound state sizes. The finite-temperature Gibbs ensemble is discuss in Fig. 3 (g), focusing on $\beta = 1/2$ and $\beta = 1$ (the different histograms in the panel). Only results for $\rho_1(x)$, for a chain with $L = 30$ are presented. The infinite temperature histogram is reported for comparison. The continuous lines are now the analytic results obtained by solving the finite-temperature TBA equations and perfectly agree with the Monte Carlo data. Upon lowering the temperature the height of the peak at $x = 0$ increases. This reflects that at $\beta = \infty$ the tail of the root distributions vanish exponentially, whereas for $\beta = 0$ they are $\sim 1/x^4$.

Finally, panels (d)-(f) plot $\rho_n(x)$ for the GGE ensemble. Specifically, we focus on the TGGE with the two charges $\mathcal{I}_2, \mathcal{I}_4$ with $\lambda_2 = 0$ and $\lambda_4 = 1$. In contrast with the thermal case (see (a)) ρ_1 exhibits a double peak structure. Similar to the infite-temperature Gibbs ensemble ((a)-(c) in the Figure), the data suggest that for $L = 30$ finite-size effects are negligible, at least for $-2 \leq x \leq 2$.

VI. CONCLUSIONS

VII. THE STRING ROOT DENSITIES AT INFINITE TEMPERATURE

For infinite temperature the densities ρ_n are given as

$$\rho_n(x) = \frac{2}{\pi} \frac{1}{(n^2 + x^2)(x^2 + (2+n)^2)} \tag{8}$$

Notice that

$$\int_{-\infty}^{+\infty} \rho_n(x) dx = \frac{1}{n(n+1)(n+2)} \tag{9}$$

Icluding the first order correction to the infinite temperature result one obtains

$$\rho_n(x) = \frac{2}{\pi} \frac{1}{(n^2 + x^2)(x^2 + (2+n)^2)} - \frac{8}{\pi} \frac{n(n+2)}{(n^2 + x^2)^2 (x^2 + (2+n)^2)^2} J\beta + \mathcal{O}(J^2\beta^2) \tag{10}$$

[1] M. Rigol, V. Dunjko, V. Yurovsky, and M. Olshanii, Phys. Rev. Lett. **98**, 050405 (2007).

[2] S. Popescu, A. J. Short, and A. Winter, Nature Physics **2**, 754 (2006).

[3] M. Rigol, V. Dunjko, and M. Olshanii, Nature **452**, 854 (2008).
[4] A. Polkovnikov, K. Sengupta, and M. Vengalattore, Rev. Mod. Phys. **83**, 863 (2011).
[5] J. Eisert., M. Friesdorf, and C. Gogolin, arXiv:1408.5148.
[6] C. Kollath, A. M. Läuchli, and E. Altman, Phys. Rev. Lett. **98**, 180601 (2007).
[7] S. R. Manmana, S. Wessel, R. M. Noack, and A. Muramatsu, Phys. Rev. Lett. **98**, 210405 (2007).
[8] P. Calabrese and J. Cardy, J. Stat. Mech. P06008 (2007).
[9] M. Cramer, C. M. Dawson, J. Eisert, and T. J. Osborne, Phys. Rev. Lett. **100**, 030602 (2008).
[10] T. Barthel and U. Schollwöck, Phys. Rev. Lett. **100**, 100601 (2008).
[11] M. Cramer, A. Flesch, I. P. McCulloch, U. Schollwöck, and J. Eisert, Phys. Rev. Lett. **101**, 063001 (2008).
[12] M. Kollar and M. Eckstein, Phys. Rev. A **78**, 013626 (2008).
[13] A. Iucci and M. A. Cazalilla, Phys. Rev. A **80**, 063619 (2009).
[14] S. Sotiriadis, P. Calabrese, and J. Cardy, EPL **87**, 20002 (2009).
[15] G. Roux, Phys. Rev. A **79**, 021608 (2009).
[16] M. Rigol, Phys. Rev. Lett. **103**, 100403 (2009).
[17] M. Rigol, Phys. Rev. A **80**, 053607 (2009).
[18] P. Barmettler, M. Punk, V. Gritsev, E. Demler, and E. Altman, Phys. Rev. Lett. **102**, 130603 (2009).
[19] P. Barmettler, M. Punk, V. Gritsev, E. Demler, and E. Altman, New J. Phys. **12**, 055017 (2010).
[20] M. Cramer and J. Eisert, New J. Phys. **12**, 055020 (2010).
[21] A. Flesch, M. Cramer, I. P. McCulloch, U. Schollwöck, and J. Eisert, Phys. Rev. A **78**, 033608 (2008).
[22] G. Roux, Phys. Rev. A **81**, 053604 (2010).
[23] D. Fioretto and G. Mussardo, New J. Phys. **12**, 055015 (2010).
[24] G. Biroli, C. Kollath, and A. M. Läuchli, Phys. Rev. Lett. **105**, 250401 (2010).
[25] L. F. Santos and M. Rigol, Phys. Rev. E **82**, 031130 (2010).
[26] M. C. Bañuls, J. I. Cirac, and M. B. Hastings, Phys. Rev. Lett. **106**, 050405 (2011).
[27] P. Calabrese, F. H. L. Essler, and M. Fagotti, Phys. Rev. Lett. **106**, 227203 (2011).
[28] C. Gogolin, M. P. Mueller, and J. Eisert, Phys. Rev. Lett. **106**, 040401 (2011).
[29] M. Rigol and M. Fitzpatrick, Phys. Rev. A **84**, 033640 (2011).
[30] T. Caneva, E. Canovi, D. Rossini, G. E. Santoro, and A. Silva, J. Stat. Mech. (2011) P07015.
[31] L. Santos, A. Polkovnikov, and M. Rigol, Phys. Rev. Lett. **107**, 040601 (2011).
[32] A. C. Cassidy, C. W. Clark, and M. Rigol, Phys. Rev. Lett. **106**, 140405 (2011).
[33] F. H. L. Essler, S. Evangelisti, and M. Fagotti, Phys. Rev. Lett. **109**, 247206 (2012).
[34] M. A. Cazalilla, A. Iucci, and M.-C. Chung, Phys. Rev. E **85**, 011133 (2012).
[35] J. Mossel and J.-S. Caux, New J. Phys. **14** 075006 (2012).
[36] M. Rigol and M. Srednicki, Phys. Rev. Lett. **108**, 110601 (2012).
[37] J. Mossel and J.-S. Caux, J. Phys. A: Math. Theor. **45**, 255001 (2012).
[38] M. Fagotti and F. H. L. Essler, Phys. Rev. B **87**, 245107 (2013).
[39] M. Fagotti, Phys. Rev. B **87**, 165106 (2013).
[40] M. Collura, S. Sotiriadis, and P. Calabrese, Phys. Rev. Lett. **110**, 245301 (2013).
[41] J.-S. Caux and F. H. L. Essler, Phys. Rev. Lett. **110**, 257203 (2013).
[42] M. Kormos, A. Shashi, Y.-Z. Chou, J.-S. Caux, and A. Imambekov, Phys. Rev. B **88**, 205131 (2013).
[43] B. Bertini, D. Schuricht, and F. H. L. Essler, arXiv:1405.4813 (2014).
[44] S. Sotiriadis and P. Calabrese, J. Stat. Mech. (2014) P07024.
[45] F. H. L. Essler, S. Kehrein, S. R. Manmana, and N. J. Robinson, Phys. Rev. B **89**, 165104 (2014).
[46] M. Fagotti, M. Collura, F. H. L. Essler, and P. Calabrese, Phys. Rev. B **89**, 125101 (2014).
[47] M. Fagotti, J. Stat. Mech. (2014) P03016.
[120] B. Wouters, J. De Nardis, M. Brockmann, D. Fioretto, M. Rigol, and J.-S. Caux, Phys. Rev. Lett. **113**, 117202 (2014).
[119] B. Pozsgay, M. Mestyán, M. A. Werner, M. Kormos, G. ZaràND, and G. Takács, Phys. Rev. Lett. **113**, 117203 (2014).
[50] M. Greiner, O. Mandel, T. Hänsch, and I. Bloch, Nature (London) **419**, 51 (2002).
[51] T. Kinoshita, T. Wenger, and D. S. Weiss, Nature (London) **440**, 900 (2008).
[52] S. Hofferberth, I. Lesanovsky, B. Fischer, T. Schumm, and J. Schiedmayer, Nature (London) **449**, 324 (2007).
[53] I. Bloch, J. Dalibard, and W. Zwerger, Rev. Mod. Phys. **80**, 885 (2008).
[54] S. Trotzky, Y.-A. Chen, A. Flesch, I. P. McCulloch, U. Schollwöck, J. Eisert, and I. Bloch, Nature Phys. **8**, 325 (2012).
[55] M. Gring, M. Kuhnert, T. Langen, T. Kitagawa, B. Rauer, M. Schreitl, I. Mazets, D. A. Smith, E. Demler, and J. Schmiedmayer, Science **337**, 6100 (2012).
[56] M. Cheneau, P. Barmettler, D. Poletti, M. Endres, P. Schaua, T. Fukuhara, C. Gross, I. Bloch, C. Kollath, and S. Kuhr, Nature (London) **481**, 484 (2012).
[57] U. Schneider, L. Hackeruller, J. P. Ronzheimer, S. Will, S. Braun, T. Best, I. Bloch, E. Demler, S. Mandt, D. Rasch, and A. Rosch, Nature Phys. **8**, 213 (2012).
[58] M. Kuhnert, R. Geiger, T. Langen, M. Gring, B. Rauer, T. Kitagawa, E. Demler, D. Adu Smith, and J. Schmiedmayer, Phys. Rev. Lett. **110**, 090405 (2013).
[59] T. Langen, R. Geiger, M. Kuhnert, B. Rauer, and J. Schmiedmayer, Nature Phys. **9**, 640 (2013).
[60] F. Meinert, M. J. Mark, E. Kirilov, K. Lauber, P. Weinmann, A. J. Daley, and H.-C. Nagerl, Phys. Rev. Lett. **111**, 053003 (2013).
[61] T. Fukuhara, A. Kantian, M. Endres, M. Cheneau, P. Schaua, S. Hild, C. Gross, U. Schollwöck, T. Giamarchi, I. Bloch, and S. Kuhr, Nature Phys. **9**, 235 (2013).
[62] J. P. Ronzheimer, M. Schreiber, S. Braun, S. S. Hodgman, S. Langer, I. P. McCulloch, F. Heidrich-Meisner, I. Bloch, and U. Schneider, Phys. Rev. Lett. **110**, 205301 (2013).
[63] S. Braun, M. Friesdorf, S. Hodgman, M. Schreiber, J. Ronzheimer, A. Riera, M. del Rey, I. Bloch, J. Eisert, and U. Schneider, arXiv:1403.7199.
[64] J. M. Deutsch, Phys. Rev. A **43**, 2046 (1991).
[65] M. Srednicki, Phys. Rev. E **50**, 888 (1994).
[66] M. Srednicki, J. Phys. A **29**, L75 (1996).
[67] M. Srednicki, J. Phys. A **32**, 1163 (1999).
[68] S. Goldstein, J. L. Lebowitz, R. Tumulka, and N. Zanghí, Phys. Rev. Lett. **96**, 050403 (2006).
[69] S. Goldstein, J. L. Lebowitz, C. Mastrodonato, R. Tumulka, and N. Zanghi, Proc. R. Soc. A **466**, 3203 (2010).
[70] S. Goldstein, J. L. Lebowitz, R. Tumulka, and N. Zanghi, Eur. Phys. J. H **35**, 173 (2010).
[71] T. N. Ikeda, Y. Watanabe, and M. Ueda, Phys. Rev. E **84**, 021130 (2011).
[72] T. N. Ikeda, Y. Watanabe, and M. Ueda, Phys. Rev. E **87**, 012125 (2013).
[73] R. Steinigeweg, J. Herbrych, and P. Prelovšek, Phys. Rev. E **87**, 012118 (2013).

[74] W. Beugeling, R. Moessner, and M. Haque, Phys. Rev. E **89**, 042112 (2014).
[75] R. Steinigeweg, A. Khodja, H. Niemeyer, C. Gogolin, and J. Gemmer, Phys. Rev. Lett. **112**, 130403 (2014).
[76] S. Sorg, L. Vidmar, L. Pollet, and F. Heidrich-Meisner, arXiv:1405.5404v2.
[77] W. Beugeling, R. Moessner, and M. Haque, arXiv:1407.2043.
[78] V. Khemani, A. Chandran, H. Kim, and S. L. Sondhi, arXiv:1406.4863.
[79] H. Kim, T. N. Ikeda, and D. Huse, arXiv:1408.0535.
[80] L. Bonnes, F. H. L. Essler, and A. M. Läuchli, arXiv:1404.4062 (2014).
[81] J.-S. Caux and J. Mossel, J. Stat. Mech. (2011) P02023.
[82] V. Alba, M. Fagotti, and P. Calabrese, J. Stat. Mech. (2009) P10020.
[83] N. Kitanine, J. M. Maillet, and V. Terras, Nucl. Phys. B **554**, 647 (1999).
[84] N. Kitanine, J. M. Maillet, and V. Terras, Nucl. Phys. B **567**, 554 (2000).
[85] L. Amico, R. Fazio, A. Osterloh, and V. Vedral, Rev. Mod. Phys. **80**, 517 (2008).
[86] M. Takahashi, *Thermodynamics of one-dimensional solvable models*, Cambridge University Press 1999.
[87] C. N. Yang and C. P. Yang, J. Math. Phys. **10**, 1115 (1969).
[88] M. Takahashi, Prog. Theor. Phys. **46**, 401 (1971).
[89] M. P. Grabowski and P. Mathieu, Ann. Phys. N.Y. **243**, 299 (1995).
[90] J. Eisert, M. Cramer, and M. B. Plenio, Rev. Mod. Phys. **82**, 277 (2009).
[91] P. Calabrese, J. Cardy, and B. Doyon Eds., Special issue: Entanglement entropy in extended systems, J. Phys. A **42**, 50 (2009).
[92] P. Calabrese and J. Cardy, J. Phys. A **42** 504005 (2009).
[93] V. E. Korepin, N. M. Bogoliubov, and A. G. Izergin, *Quantum Inverse Scattering Methods and Correlation Functions*, Cambridge University Press 1997.
[94] X. Zotos and P. Prelovšek, Phys. Rev. B **53**, 983 (1996).
[95] H. Castella and X. Zotos, Phys. Rev. B **54**, 4375 (1996).
[96] X. Zotos, F. Naef, and P. Prelovšek, Phys. Rev. B **55**, 11029 (1997)
[97] F. C. Alcaraz, M. I. Berganza, and G. Sierra, Phys. Rev. Lett. **106**, 201601 (2011).
[98] I. Pizorn, arXiv:1202.3336.
[99] M. I. Berganza, F. C. Alcaraz, and G. Sierra, J. Stat. Mech. (2012) P01016.
[100] G. Wong, I. Klich, L. A. P. Zayas, and D. Vaman, JHEP **12** (2013) 020.
[101] M. Storms, and R. R. P. Singh, Phys. Rev. E **89**, 012125 (2014).
[102] R. Berkovits, Phys. Rev. B **87**, 075141 (2013).
[103] F. H. L. Essler, A. M. Läuchli, and P. Calabrese, Phys. Rev. Lett. **110**, 115701 (2013).
[104] M. Nozaki, T. Numasawa, T. Takayanagi, Phys. Rev. Lett. **112**, 111602 (2014).
[105] G. Ramirez, J. Rodriguez-Laguna, and G. Sierra, arXiv:1402.5015.
[106] F. Ares, J. G. Esteve, F. Falceto, and E. Sánchez-Burillo, arXiv:1401.5922.
[107] Y. Huang, and J. Moore, arXiv:1405.1817.
[108] T. Pálmai, arXiv:1406.3182.
[109] J. Mölter, T. Barthel,U. Schollwöck, and V. Alba, arXiv:1407.0066.
[110] H.-H. Lai and K. Yang, arXiv:1409:1224
[111] J. Sato, B. Aufgebauer, H. Boos, F. Göhmann, A. Klümper, M. Takahashi, and C. Trippe, Phys. Rev. Lett. **106**, 257201 (2011).
[112] M. Fagotti and P. Calabrese, Phys. Rev. A **78**, 010306 (2008).
[113] V. Gurarie, J. Stat. Mech. (2014) P02014.
[114] M. Collura, M. Kormos, and P. Calabrese, J. Stat. Mech. (2014) P01009.
[115] M. Kormos, L. Bucciantini, and P. Calabrese, EPL **107**, 40002 (2014).
[116] J.-S. Caux and J.-M. Maillet, Phys. Rev. Lett. **95**, 077201 (2005).
[117] J.-S. Caux, R. Hagemans and J.-M. Maillet, J. Stat. Mech. P09003 (2005).
[118] J.-S. Caux, J. Math. Phys. **50**, 095214 (2009).
[119] B. Pozsgay, M. Mestyán, M. A. Werner, M. Kormos, G. Zaránd, and G. Takács, Phys. Rev. Lett. **113**, 117203 (2014).
[120] B. Wouters, M. Brockmann, J. De Nardis, D. Fioretto, M. Rigol, and J.-S. Caux, Phys. Rev. Lett. **113**, 117202 (2014).
[121] S.-J. Gu, N. M. R. Peres, Y.-Q. Li, Eur. Phys. J. B **48**, 157 (2005).